

deadtrees.earth - An Open-Access and Interactive Database for Centimeter-Scale Aerial Imagery to Uncover Global Tree Mortality Dynamics

Clemens Mosig^{*1,2}, Janusch Vajna-Jehle^{*3}, Miguel D. Mahecha^{1,2,4}, Yan Cheng⁵, Henrik Hartmann^{6,7,8}, David Montero^{1,4}, Samuli Junttila⁹, Stéphanie Horion⁵, Mirela Beloiu Schwenke¹⁰, Stephen Adu-Bredu¹¹, Djamil Al-Halbouni¹, Matthew Allen¹², Jan Altman^{13,14}, Claudia Angiolini¹⁵, Rasmus Astrup¹⁶, Caterina Barrasso^{2,17}, Harm Bartholomeus¹⁸, Benjamin Brede¹⁹, Allan Buras²⁰, Erik Carrieri²¹, Gherardo Chirici²², Myriam Cloutier²³, KC Cushman²⁴, James W. Dalling²⁵, Jan Dempewolf²⁶, Martin Denter²⁷, Simon Ecke^{28,26}, Jana Eichel²⁹, Anette Eltner³⁰, Maximilian Fabi³, Fabian Fassnacht³¹, Matheus Pinheiro Feirreira³², Julian Frey²⁸, Annett Frick³³, Selina Ganz^{3,34}, Matteo Garbarino²¹, Milton García³⁵, Matthias Gassilloud³, Marziye Ghasemi³⁶, Francesca Giannetti²², Roy Gonzalez³⁷, Carl Gosper³⁸, Konrad Greinwald³⁹, Stuart Grieve^{40,41}, Jesus Aguirre Gutierrez^{42,43}, Anna Göritz³, Peter Hajek³⁹, David Hedding⁴⁴, Jan Hempel¹, Melvin Hernández³⁵, Marco Heurich^{45,46,47}, Eija Honkavaara⁴⁸, Tommaso Jucker⁴⁹, Jesse M. Kalwij^{50,51}, Pratima Khatri-Chhetri⁵², Hans-Joachim Klemmt²⁶, Niko Koivumäki⁴⁸, Kirill Korznikov¹³, Stefan Kruse⁵³, Robert Krüger³⁰, Etienne Laliberté²³, Liam Langan⁵⁴, Hooman Latifi³⁶, Jan Lehmann⁵⁵, Linyuan Li⁵⁶, Emily Lines¹², Javier Lopatin^{57,58,59}, Arko Lucieer⁶⁰, Marvin Ludwig⁵⁵, Antonia Ludwig¹, Päivi Lyytikäinen-Saarenmaa⁴⁸, Qin Ma⁶¹, Giovanni Marino⁶², Michael Maroschek^{63,20}, Fabio Meloni²¹, Annette Menzel²⁰, Hanna Meyer⁵⁵, Mojdeh Miraki⁶⁴, Daniel Moreno-Fernández^{65,66}, Helene C. Muller-Landau³⁵, Mirko Mälicke^{67,68}, Jakobus Möhring¹, Jana Müllerova⁶⁹, Paul Neumeier¹, Roope Näsi⁴⁸, Lars Oppgenorth⁷⁰, Melanie Palmer⁷¹, Thomas Paul⁷², Alastair Potts⁷³, Suzanne Prober⁷⁴, Stefano Puliti¹⁶, Oscar Pérez-Priego⁷⁵, Chris Reudenbach⁷⁰, Christian Rossi⁷⁶, Nadine Katrin Ruehr⁷⁷, Paloma Ruiz-Benito⁶⁵, Christian Mestre

Runge⁷⁰, Michael Scherer-Lorenzen³⁹, Felix Schiefer⁵⁰, Jacob Schladebach⁵³, Marie-Therese Schmehl⁷⁸, Selina Schwarz⁷⁷, Rupert Seidl^{20,63}, Elham Shafeian⁷⁹, Leopoldo de Simone⁸⁰, Hormoz Sohrabi⁶⁴, Laura Sotomayor⁶⁰, Ben Sparrow^{81,82}, Benjamin S.C. Steer⁷¹, Matt Stenson⁷⁴, Benjamin Stöckigt³³, Yanjun Su⁸³, Juha Suomalainen⁴⁸, Michele Torresani⁸⁴, Josefine Umlauf², Nicolás Vargas-Ramírez⁸⁵, Michele Volpi⁸⁶, Vicente Vásquez⁸⁷, Ben Weinstein⁸⁷, Tagle Casapia Ximena^{18,88}, Katherine Zdunic³⁸, Katarzyna Zielewska-Büttner⁸⁹, Raquel Alves de Oliveira⁴⁸, Liz van Wagtenonk⁵², Vincent von Dosky⁹⁰, and Teja Kattenborn³

¹Institute for Earth System Science and Remote Sensing, Leipzig University, Germany

²Earth and Environmental Sciences Group, Center for Scalable Data Analytics and Artificial Intelligence (ScaDS.AI), Germany

³Department of Sensor-based Geoinformatics, University of Freiburg, Germany

⁴German Center for Integrative Biodiversity Research (iDiv), Germany

⁵Department of Geosciences and Natural Resource Management, University of Copenhagen, Denmark

⁶Institute for Forest Protection, Julius Kühn Institute (JKI) - Federal Research Centre for Cultivated Plants, Germany

⁷Faculty of Forest sciences and Forest Ecology, Georg-August-University Göttingen, Germany

⁸Department of Biogeochemical Processes, Max Planck Institute for Biogeochemistry, Germany

⁹School of Forest Sciences, University of Eastern Finland, Finland

¹⁰Department of Environmental Systems Sciences, ETH Zurich, Switzerland

¹¹CSIR-Forestry Research Institute of Ghana, Ghana

¹²Department of Geography, University of Cambridge, United Kingdom

¹³Department of Functional Ecology, Institute of Botany of the Czech Academy of Sciences, Czechia

¹⁴Faculty of Forestry and Wood Sciences, Czech University of Life Sciences, Czechia

¹⁵National Biodiversity Future Center (NBFC), Italy

- ¹⁶Norwegian Institute of Bioeconomy Research (NIBIO), Norway
- ¹⁷Chair of Computational Landscape Ecology, Dresden University of Technology (TUD),
Germany
- ¹⁸Laboratory for Geo-Information Science and Remote Sensing, Wageningen University,
Netherlands
- ¹⁹Section 1.4 Remote Sensing and Geoinformatics, GFZ German Research Centre for
Geosciences, Germany
- ²⁰TUM School of Life Sciences, Technical University of Munich, Germany
- ²¹University of Turin, Italy
- ²²GeoLAB Laboratory of Forest Geomatics, Department of Agriculture, Food, Environment
and Forestry, University of Florence, Italy
- ²³Département de sciences biologiques, Université de Montréal, Canada
- ²⁴Environmental Sciences Division, Oak Ridge National Laboratory, USA
- ²⁵University of Illinois, USA
- ²⁶Bavarian State Institute of Forestry, Germany
- ²⁷Chair of Remote Sensing and Landscape Information Systems, University of Freiburg,
Germany
- ²⁸Chair of Forest Growth and Dendroecology, University of Freiburg, Germany
- ²⁹Department of Physical Geography, Utrecht University, Netherlands
- ³⁰Institute of Photogrammetry and Remote Sensing, Dresden University of Technology
(TUD), Germany
- ³¹Institute of Geographical Sciences, Freie Universität Berlin, Germany
- ³²Dept. of Forest Sciences, 'Luiz de Queiroz' College of Agriculture (ESALQ), University
of São Paulo (USP), Brazil
- ³³Luftbild Umwelt Planung GmbH (LUP), Germany
- ³⁴Department of Biometry and Informatics, Forest Research Institute (FVA), Germany
- ³⁵Smithsonian Tropical Research Institute, Panama
- ³⁶Department of Photogrammetry and Remote Sensing, K. N. Toosi University of
Technology, Iran
- ³⁷University of Tolima, Colombia

- ³⁸Biodiversity and Conservation Science, Western Australian Department of Biodiversity, Conservation and Attractions, Australia
- ³⁹Chair of Geobotany, Faculty of Biology, University of Freiburg, Germany
- ⁴⁰School of Geography, Queen Mary University of London, United Kingdom
- ⁴¹Digital Environment Research Institute, Queen Mary University of London, UK
- ⁴²Environmental Change Institute, School of Geography and the Environment, University of Oxford, University of Oxford, UK
- ⁴³Leverhulme Centre for Nature Recovery, University of Oxford, UK
- ⁴⁴Department of Geography, University of South Africa, South Africa
- ⁴⁵Department of National Park Monitoring and Animal Management, Bavarian Forest National Park, Germany
- ⁴⁶Inland Norway University of Applied Science, Norway
- ⁴⁷Chair of Wildlife Ecology and Wildlife Management, University of Freiburg, Germany
- ⁴⁸Department of Remote Sensing and Photogrammetry, Finnish Geospatial Research Institute, National Land Survey of Finland, Finland
- ⁴⁹School of Biological Sciences, University of Bristol, UK
- ⁵⁰Institute of Geography and Geoecology, Karlsruhe Institute of Technology (KIT), Germany
- ⁵¹Centre for Ecological Genomics & Wildlife Conservation, Department of Zoology, University of Johannesburg, South Africa
- ⁵²School of Environmental and Forest Sciences, University of Washington, USA
- ⁵³Polar Terrestrial Environmental Systems, Alfred Wegener Institute, Germany
- ⁵⁴Quantitative Biogeography, Senckenberg Biodiversity and Climate Research Centre (SBiK-F), Germany
- ⁵⁵Institute of Landscape Ecology, University of Münster, Germany
- ⁵⁶College of Forestry, Beijing Forestry University, China
- ⁵⁷Facultad de Ingeniería y Ciencias, Universidad Adolfo Ibáñez, Chile
- ⁵⁸Data Observatory Foundation, ANID Technology Center No. DO210001, Chile
- ⁵⁹Center for Climate Resilience Research (CR)2, University of Chile, Chile
- ⁶⁰School of Geography, Planning and Spatial Sciences, University of Tasmania, Australia

- ⁶¹School of Geography, Nanjing Normal University, China
- ⁶²Institute for Sustainable Plant Protection, National Research Council of Italy, Italy
- ⁶³Research and Monitoring, Nationalpark Berchtesgaden, Germany
- ⁶⁴Department of Forest Science and Engineering, Tarbiat Modares University, Iran
- ⁶⁵Departamento de Ciencias de la Vida, Universidad de Alcalá, Spain
- ⁶⁶Institute of Forest Sciences (INIA-CSIC), Spain
- ⁶⁷Institute for Water and Environment - Hydrology, Karlsruhe Institute of Technology (KIT), Germany
- ⁶⁸hydrocode GmbH, Karlsruhe, Germany, Germany
- ⁶⁹Institute of Botany, Academy of Sciences of the Czech Republic, Czechia
- ⁷⁰Universität Marburg, Germany
- ⁷¹Data and Geospatial Intelligence, Scion Research, New Zealand
- ⁷²Forest Ecology and Management, Scion Research, New Zealand
- ⁷³Spekboom Restoration Research Group, Nelson Mandela University, South Africa
- ⁷⁴Environment, Commonwealth Scientific and Industrial Research Organisation, Australia
- ⁷⁵Department of Forestry Engineering, University of Cordoba, Spain
- ⁷⁶Swiss National Park, Switzerland
- ⁷⁷KIT-Campus Alpin, Karlsruhe Institute of Technology (KIT), Germany
- ⁷⁸Department of Hydrology and Climatology, Potsdam University, Germany
- ⁷⁹Department of Soil Science, University of Saskatchewan, Canada
- ⁸⁰Department of Life Sciences, University of Siena, Italy
- ⁸¹School of Biological Sciences, The University of Adelaide, Australia
- ⁸²Terrestrial Ecosystem Research Network (TERN), Australia
- ⁸³State Key Laboratory of Vegetation and Environmental Change, Institute of Botany, Chinese Academy of Sciences, China
- ⁸⁴Faculty of Agricultural, Environmental and Food science, Free University of Bozen-Bolzano, Italy
- ⁸⁵Center for Multidisciplinary Research on Chiapas and the Southern Border, National Autonomous University of Mexico, Mexico
- ⁸⁶Swiss Data Science Center, ETH Zurich and EPFL, Switzerland

⁸⁷School of Forestry, Fisheries and Geomatics, University of Florida, USA

⁸⁸Forest Program, Instituto de Investigaciones de la Amazonia Peruana (IIAP), Peru

⁸⁹Department of Forest Nature Conservation, Forest Research Institute (FVA), Germany

⁹⁰unique land use GmbH, Germany

*Shared first authorship: clemens.mosig@uni-leipzig.de,

janusch.jehle@geosense.uni-freiburg.de

October 20, 2024

Abstract

Excessive tree mortality is a global concern and remains poorly understood as it is a complex phenomenon. We lack global and temporally continuous coverage on tree mortality data. Ground-based observations on tree mortality, *e.g.*, derived from national inventories, are very sparse, not standardized and not spatially explicit. Earth observation data, combined with supervised machine learning, offer a promising approach to map tree mortality over time. However, global-scale machine learning requires broad training data covering a wide range of environmental settings and forest types. Drones provide a cost-effective source of training data by capturing high-resolution orthophotos of tree mortality events at sub-centimeter resolution. Here, we introduce deadtrees.earth, an open-access platform hosting more than a thousand centimeter-resolution orthophotos, covering already more than 300,000 ha, of which more than 58,000 ha are fully annotated. This community-sourced and rigorously curated dataset shall serve as a foundation for a global initiative to gather comprehensive reference data. In concert with Earth observation data and machine learning it will serve to uncover tree mortality patterns from local to global scales. This will provide the foundation to attribute tree mortality patterns to environmental changes or project tree mortality dynamics to the future. Thus, the open and interactive nature of deadtrees.earth together with the collective effort of the community is meant to continuously increase our capacity to uncover and understand tree mortality patterns.

1 Introduction

2 In recent decades, elevated tree mortality rates have been reported for many regions of the world
3 (Hartmann et al. 2022). This phenomenon is attributed to climate change-induced more frequent and
4 intense climate extremes such as droughts, heatwaves, and late frosts, that often trigger outbreaks of

5 damaging insects or epidemic diseases (Anderegg et al. 2013; Bauman et al. 2022; Gora and Esquivel-
6 Muelbert 2021; Hartmann et al. 2022; Senf et al. 2020; Trumbore et al. 2015). Tree mortality is
7 generally not driven by a single driver but by complex compound events, consisting of multiple biotic
8 and abiotic agents and feedbacks (Allen et al. 2010; Bastos et al. 2023; Mahecha et al. 2024). This
9 may include a combination of consecutive heatwaves, meteorological and soil droughts, followed by
10 late frosts after leaf budding, and the infestation of already weakened trees by pest and pathogens
11 (Coleman et al. 2018; Fettig et al. 2019; Stephenson et al. 2019; Trugman et al. 2021).

12 Trees are long-lived and sessile organisms that cannot escape extreme conditions via migration,
13 and their capacity to acclimate or adapt evolutionary to rapid environmental changes is slow (Allen
14 et al. 2015). Accordingly, the spatio-temporal patterns of standing dead tree canopies are direct indi-
15 cators of how different tree species, functional types, ages, or entire ecosystems cope with biotic and
16 abiotic stressors (Anderegg et al. 2013; Hartmann et al. 2022). Moreover, timely information on tree
17 mortality dynamics is urgently needed by decision-makers in forest management and nature conser-
18 vation. Information on tree mortality patterns is required to identify adaptation strategies, including
19 selecting tree species, optimizing harvesting cycle, managing pest and disease outbreaks (*e.g.*, bark
20 beetle), ensure the provision of ecosystem services and controlling fuel accumulation for wildfire risk
21 reduction (Garrity et al. 2013; Moghaddas et al. 2018; Stephens et al. 2018, 2022; Vilanova et al.
22 2023; Winter et al. 2024). Moreover, tracking tree mortality patterns helps indicate where ecosystems
23 are undergoing rapid compositional transformations, *i.e.*, shift in species and their role in the terres-
24 trial carbon cycle, *e.g.*, via declining net carbon sinks (Hill et al. 2023; Pan et al. 2011; Scheffer et al.
25 2001; Stephens et al. 2022).

26 Despite its importance, the extent and rate of tree mortality at the global scale remains largely
27 unknown or imprecise (Allen et al. 2015). Although ground-based inventories are the gold standard
28 in forestry, national forest inventories only sometimes record tree mortality, but usually have sparse
29 spatial coverage (Puletti et al. 2019) and low temporal sampling frequencies (*e.g.*, 10-year intervals),
30 which do not align well with the rapid dynamics of environmental stressors. Therefore, these inven-
31 tories provide limited assistance in attributing tree mortality to short-term environmental dynamics
32 such as climate extremes or insect outbreaks (Hülsmann et al. 2017; Woodall et al. 2005). Conse-
33 quently, meta-analyses based on such ground observations could be biased or underrepresented for
34 recent elevated tree mortality (Hammond et al. 2022; Yan et al. 2024). The value of field inventories
35 for global tree mortality studies is further complicated by the commonly low data accessibility and

36 heterogeneity in sampling protocols and data quality (McRoberts et al. 2010; Senf et al. 2018). Recent
37 initiatives such as the global tree mortality database (Hammond et al. 2022) have gathered and har-
38 monized invaluable information towards a global assessment of tree mortality. However, they are still
39 severely limited in their spatial and temporal coverage and are not based on a systematic assessment
40 that would enable scaling to larger spatial scales. Uncovering global tree mortality patterns requires a
41 multi-faceted approach that complements the ground-based assessments.

42 Satellite-based Earth Observation offers a promising avenue, providing seamless spatial coverage
43 and temporally consistent monitoring (The International Tree Mortality Network et al. 2024). Using
44 data from the Landsat satellite mission, Hansen *et al.* created the prominent global *forest loss* map by
45 applying a decision tree classifier on time series of spectral metrics (Hansen et al. 2013). However,
46 this approach reveals a binary classification of forest loss, not tree mortality, and is restricted to 30 m
47 spatial resolution and thus cannot detect the often scattered patterns of tree mortality (Cheng et al.
48 2024; Espírito-Santo et al. 2014; Schiefer et al. 2024). Unsupervised approaches, that is analysis
49 without labeled reference data, can reveal continuous forest responses using anomalies of vegetation
50 indices, which are computed by combining multiple spectral bands for each pixel (Lange et al. 2024;
51 Senf and Seidl 2021; Senf et al. 2018, 2020; Thonfeld et al. 2022). However, vegetation indices
52 cannot directly reveal tree mortality and using such methods to uncover scattered and small-scale
53 mortality remains a challenging task. Therefore, translating the complex Earth observation signals to
54 tree mortality patterns requires a supervised approaches (Schiefer et al. 2023).

55 The Earth observation community, thus, currently lacks a representative collection of reference
56 data for training and validating supervised methods for monitoring tree mortality. Given the relatively
57 coarse resolution, satellite data does not provide the necessary spatial detail to extract such reference
58 data directly. Airplane aerial images typically have higher resolutions and are often freely available for
59 regions or entire countries and, therefore, provide a promising source to map tree mortality (Cheng
60 et al. 2024; Junttila et al. 2024; Schwarz et al. 2024). However, airplane imagery are only openly
61 available in few countries and their spatial resolutions typically range from 20-60 cm, in rare cases up
62 to 10 cm. This can be a critical constrain to uncover tree mortality, as an image resolution of 20 cm or
63 less does not always enable most precise differentiation of dead from alive tree crowns and may lead
64 to missing small dead trees (compare [Figure 1](#)). For some species, crown shapes, or sizes, mortality is
65 still clearly visible at 60 cm and in studies that are limited to specific ecosystems, *e.g.*, with dominantly
66 coniferous species, coarse aerial images suffice (Junttila et al. 2024). Such resolution does not suffice,

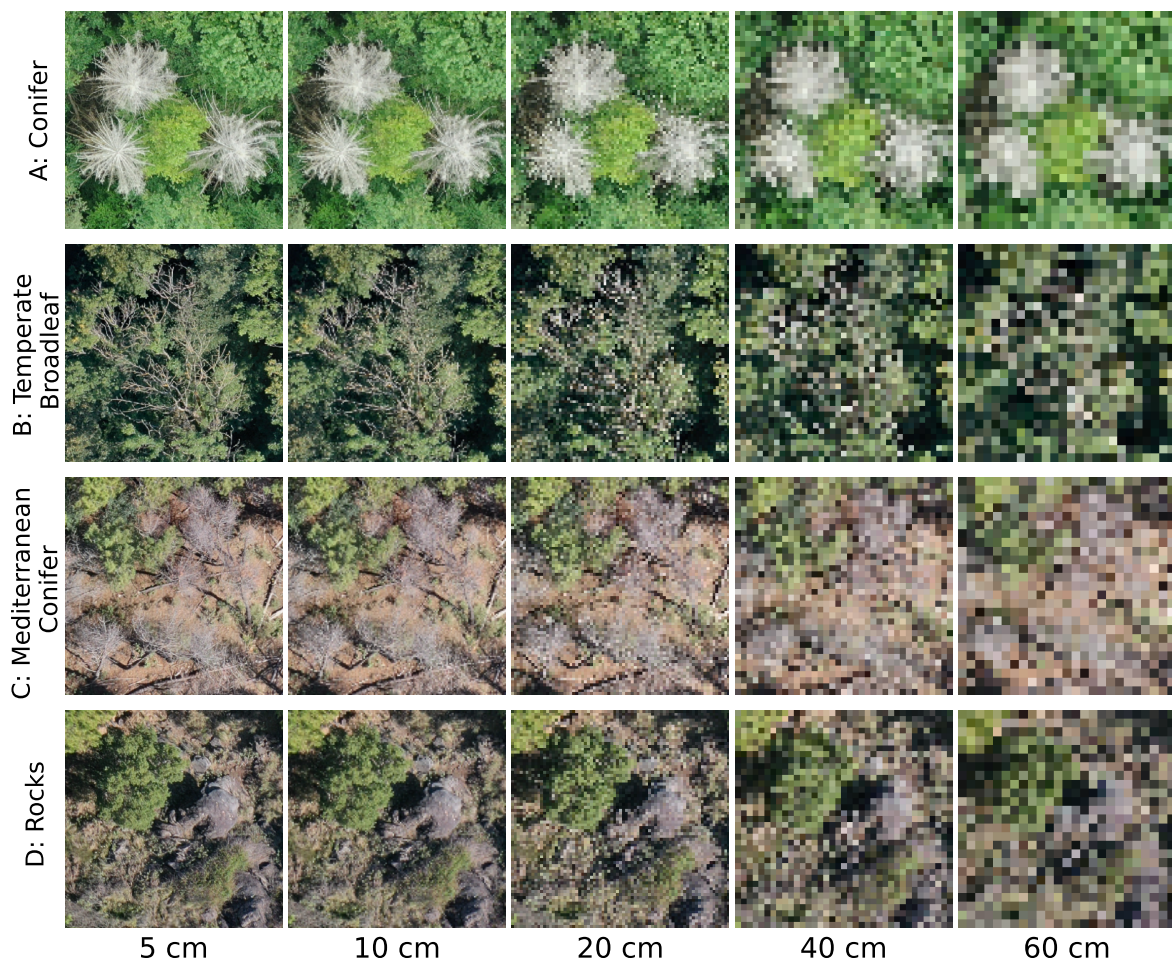


Figure 1: Four forest sites, 15 m in width and height and at resolutions of 5 cm to 60 cm. From top to bottom (*A* to *C*), the tree species are *Picea abies*, *Fraxinus excelsior*, and *Pinus sylvestris*. Row *D* shows an example where rocks cannot be distinguished from deadwood in coarse-resolution images. The original images have resolutions better than 5 cm and were resampled (nearest-neighbor) for this visualization. Airplane images at the same resolution commonly appear less clear at similar resolutions, hence these images are best-case scenarios.

67 to accurately reveal partial dieback of broadleaf trees (row *B* in Figure 1), mortality atop a bright
68 forest floor (row *C* in Figure 1), or in the presence of objects such as rocks that have a geometry that
69 is similar to tree crowns (*e.g.*, rocks, row *D* in Figure 1). Hence, to achieve accurate reference data
70 across all ecosystems and tree types a finer resolution in the centimeter range (≤ 10 cm) is needed,
71 calling for a representative global collection of centimeter-scale imagery.

72 Drones are becoming increasingly accessible and require minimal training for operation (P. John-
73 son et al. 2017; Rossi and Wiesmann 2024; Tang and Shao 2015). Suitable orthophotos for precise tree
74 mortality identification at the centimeter scale can be obtained by non-technical users with consumer-
75 type drones and easy-to-use mapping apps. In a recent case study in Germany, Schiefer et al. (2023)

76 leveraged high-resolution drone aerial images (4 cm resolution) as reference to infer the fractional
77 cover of standing deadwood [%] in pixels of satellite data (Sentinel-1 and -2). However, drones re-
78 quire operators to go into the field, creating significant labor costs and time investment. Hence, lever-
79 aging drone orthophotos for use in global tree mortality monitoring can only be achieved through a
80 large collective effort across institutions, researchers, and citizens across the globe, to finally acquire
81 a rich collection of orthophotos to represent all forest ecosystems.

82 Here, we introduce [deadtrees.earth](#), an open science, collaborative platform for accessing, shar-
83 ing, analyzing, and visualizing a global database of orthophotos with labeled standing deadwood.
84 The [deadtrees.earth](#) platform features open-access interactive functionality, allowing users to upload
85 and download images and labels through the website and an API. It also incorporates expert qual-
86 ity control workflows to maintain high data standards. This collection, across spatial and temporal
87 scales, offers unparalleled opportunities for researchers to advance satellite-based model training and
88 validation. The platform's backend is built with a scalable architecture to allow growth into a large
89 machine learning model ecosystem. Beyond machine-learning applications, this database also enables
90 verification of existing products. Contributors are acknowledged for their data contributions, fostering
91 transparent community participation and acknowledgment.

92 **2 The deadtrees.earth platform**

93 [deadtrees.earth](#) is a dynamic, community-built, open-access database for aerial orthophotos of delin-
94 eated standing deadwood. This section presents our definition of standing deadwood, the database
95 structure, database statistics, and a web platform for the integration of the database into the commu-
96 nity.

97 **2.1 Standing Deadwood**

98 We focus on *standing deadwood*, defined as woody material (twigs, branches, or stems) that has
99 died off but has largely retained its original structure, including brown-stage mortality. For deciduous
100 tree that is a lack of leafs in leaf-on season, that is either in summer or in wet season ([Figure 2](#)).
101 Standing deadwood can be identified in centimeter-scale RGB images acquired by drones or airplanes
102 by methods such as semantic segmentation, which involves the generic segmentation of any dead tree
103 crown or branch (Schiefer et al. 2023), or instance segmentation, where each segment corresponds to

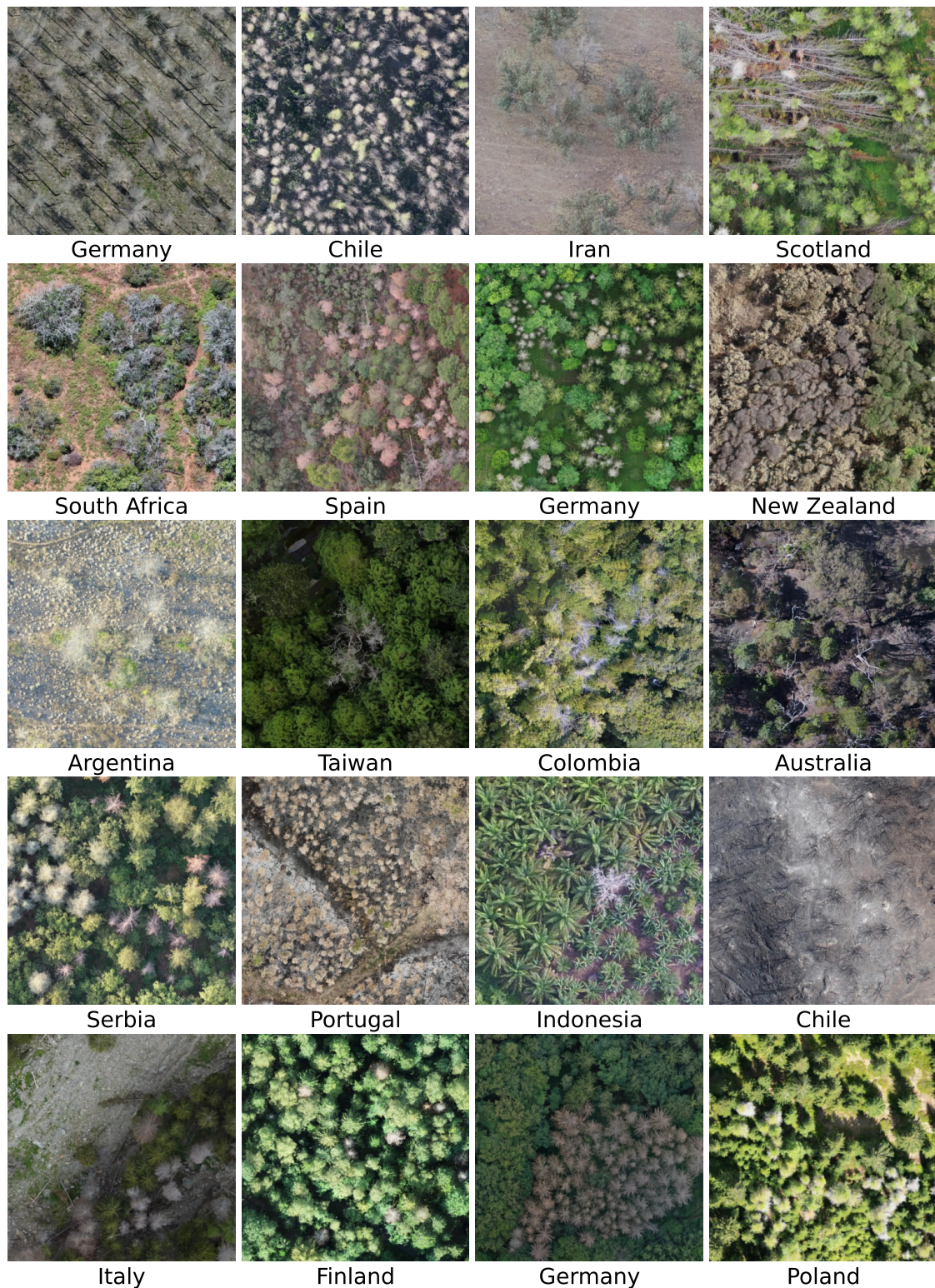


Figure 2: Sample image sections of standing and lying deadwood in a variety of contexts. The caption below each image denotes the acquisition location of the drone orthophoto. All images are available in the database.

104 an individual tree crown (Cheng et al. 2024).

105 Information on lying deadwood is not considered for this database. In contrast to standing dead
106 tree crowns, fallen tree stems are less likely to be detected in drone and airplane imagery, as they
107 are readily occluded by surrounding tree crowns or are rapidly covered by understory. Additionally,
108 fallen trees can be several decades old and are hence less interesting for studying tree mortality as a
109 response to recent environmental changes, climate extremes, or pests and pathogens.

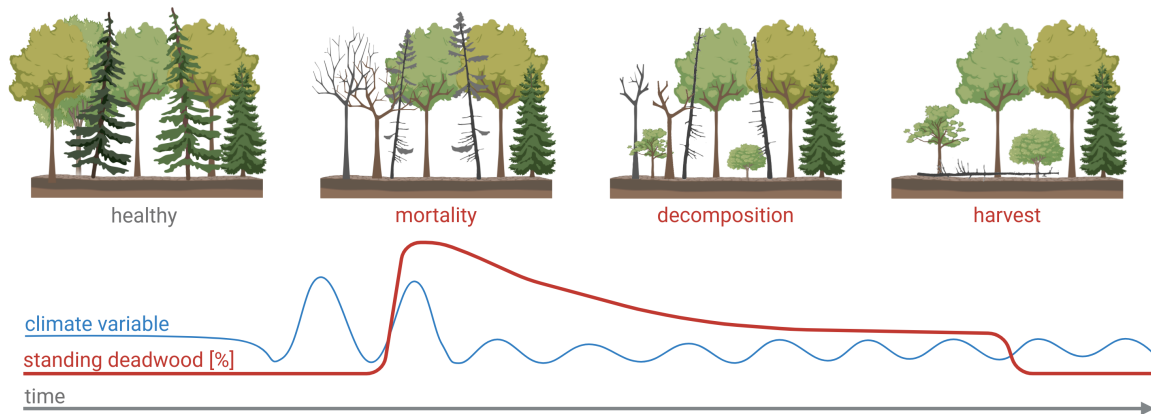


Figure 3: Temporal signature of standing deadwood (red) in multiple scenarios. Climate extreme events (blue) cause tree mortality to increase. Natural decomposition and/or harvesting/salvaging decreases standing deadwood.

110 The amount of standing deadwood changes over time with different events (Figure 3). Climate
111 extreme events, such as droughts, can cause tree mortality, increasing the amount of standing dead-
112 wood. Standing deadwood is not limited to fully dying trees; partial dieback also affects the amount
113 of standing deadwood. Explicitly including partial dieback is important, as it can be difficult to vi-
114 sually separate trees in imagery of dense forests with complex crown structures (South Africa, Iran,
115 and Australia in Figure 2). In subsequent years, standing dead trees decompose and the fraction of
116 standing deadwood decreases. As soon as dead trees fall over, are felled, or are completely removed,
117 they no longer count as standing deadwood.

118 Although the concept of standing deadwood is simple, understanding its temporal dynamics re-
119 quires several considerations. First, the falling of healthy trees does not affect the fraction of standing
120 deadwood. This also includes removing unhealthy trees that have not yet changed their appearance
121 from above and are removed before visible leaf loss. Secondly, a high amount of standing deadwood
122 in one year does not imply that those trees died that year, but several years before that is also possi-
123 ble. Note that the year of the first appearance can be extracted from a standing deadwood time series

Orthophoto Metadata:

Author: Miguel Mahecha and Clemens Mosig
Acquisition date: 3rd Sep 2023
License: CC BY
Platform: drone
Resolution: 3.4 cm

AOI Metadata:

Orthophoto quality inside AOI: 3/3

Label Set Metadata:

Author: Jan Hempel
Quality: 3/3
Type: instance segmentation
Source: manual segmentation

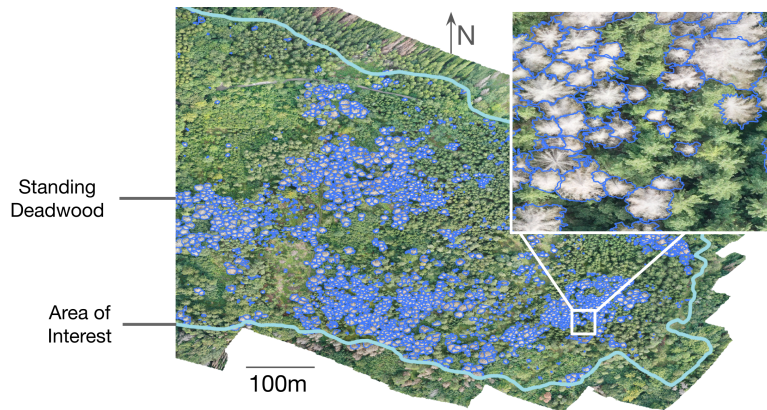


Figure 4: Sample entry of [orthophoto](#) (Jena, Germany, centroid: 50.911271°N 11.509977°W) with one label set for one area of interest (AOI) in the deadtrees.earth database. Only a simplified set of attributes are shown, see [Figure 8](#) for the precise database structure.

124 (Schiefer et al. 2024). Thirdly, drought or cold semi-deciduous species that shed their leaves during
125 climate extremes or species that resprout epicormically after disturbances such as fire, may visually
126 appear as standing deadwood at one time point but may regrow leaves at a later time, *e.g.*, red needle
127 cast (Watt et al. 2024).

128 2.2 Database Structure

129 The deadtrees.earth database is a collection of geo-referenced RGB orthophotos gathered over forests
130 with optionally one or more sets of labels depicting standing deadwood. Our database focuses on
131 airborne imagery better than 10 cm while also allowing submissions of up to 1 m for unrepresented
132 regions or where validated tree mortality labels are provided.

133 Each **orthophoto** comes with the following metadata: acquisition date, author(s), resolution, plat-
134 form, resolution and license (compare [Figure 4](#)). The author(s) can be one or multiple individuals who
135 contributed to capturing the orthophoto. The acquisition date is crucial for linking with environmen-
136 tal conditions to validate whether the orthophoto was captured in leaf-on season because one cannot
137 differentiate between dead and alive trees in orthophotos that were captured in leaf-off season. Given
138 that data contributors track the acquisition date with different accuracy, we accommodate three levels
139 of precision for the acquisition date, that is, accurate in days, months, or years. Noting the possi-
140 ble temporal error is of utmost importance when combining these observations with other datasets,
141 such as satellite time series (see [Subsection 3.2](#)). Also, for each orthophoto, the average ground sam-
142 pling distance (GSD) is automatically calculated to allow users to filter data based on different spatial

143 resolutions (see [Figure 4](#)).

144 Regardless of the spatial resolution, the information quality of an orthophoto can be constrained
145 by various factors. These constraints include poor lighting conditions (*e.g.*, underexposure), recon-
146 struction artifacts, motion blur, or data gaps (Dandois et al. 2015; Frey et al. 2018). The image con-
147 dition can vary heavily across an orthophoto, *e.g.*, image edges are often distorted. To account for
148 this, we assign each orthophoto an **area of interest (AOI)** that is a multi-polygon. This AOI object
149 includes a score noting the quality of the orthophoto inside the AOI (see [Figure 4](#)). The scoring sys-
150 tem ranges from 1 to 3, with 3 indicating near-perfect image quality, where only small portions (up to
151 5%) of the image are affected by constraints. A score of 2 is given if up to 25% of the AOI is affected,
152 while a score of 1 is assigned when up to 50% of the orthoimage inside the AOI is constrained. Both
153 the AOI and quality score are determined during a meticulous manual audit.

154 **Label sets** are polygons or points located over standing deadwood in orthophotos identified
155 through visual inspection or from automatic segmentation (Cheng et al. 2024; Junntila et al. 2024;
156 Schiefer et al. 2023). More specifically, there are four types of labels: (*i*) centroids of individual dead
157 tree crowns, (*ii*) bounding boxes of individual dead trees, (*iii*) delineations of individual dead tree
158 crowns (instance segmentation), and (*iv*) delineations around a group of adjacent dead trees or dead
159 tree parts (semantic segmentation). Each label set is associated with an AOI, that also acts as bound-
160 ary of the labeling effort. This means area inside the AOI that was not marked as deadwood can be
161 assumed to be alive or non-tree objects (see [Figure 4](#)). Lastly, there can be multiple sets of labels from
162 different sources for the same orthophoto, *e.g.*, one may have been created manually while a second
163 set was machine-generated by a segmentation model.

164 The quality of the labels will be assessed during an audit, where, again, a quality score between
165 1 and 3 will be assigned. A score of 3/3 means accurately delineated standing deadwood and partial
166 dieback (see [Figure 4](#)). In the score of 2/3 we include sets where the vast majority of deadwood is
167 labeled and/or delineations have imperfections, *e.g.*, partially include forest floor or disregard partial
168 dieback. Label sets with a score 1/3 include all other sets and are recommended to be excluded in
169 further analysis or machine learning applications.

170 **2.3 Platform architecture**

171 The [deadtrees.earth](#) platform is an integrated web-based system designed to facilitate visualization,
172 participation, management, and access to the deadtrees.earth database. The platform architecture con-

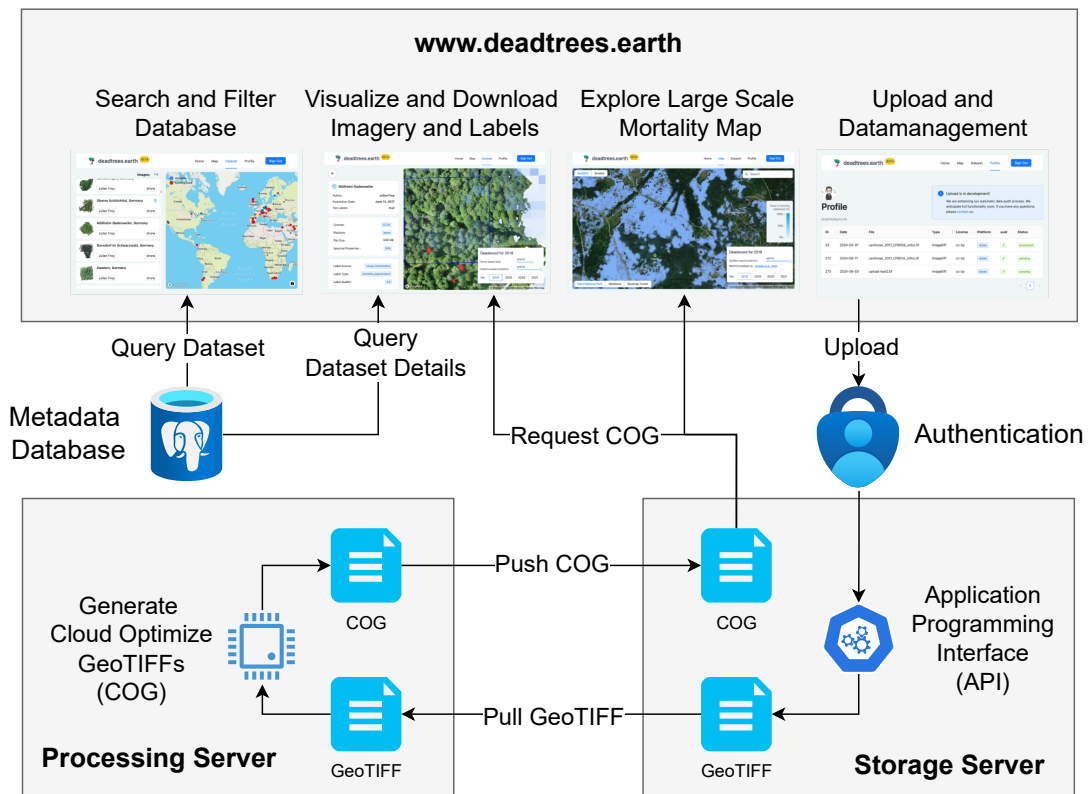


Figure 5: System diagram illustrating the main components of the deadtrees.earth platform and their interactions. Users can search and filter the database, visualize and download orthophotos, and explore a large-scale mortality map. The processing server generates Cloud Optimized GeoTIFFs (COGs) by pulling GeoTIFF files and pushing processed COGs to the storage server.

173 sists of the following components: a user-facing front-end application, a cloud-hosted database for
174 metadata and labels, a storage server for orthophotos and Cloud Optimized GeoTIFFs (COGs), a
175 processing server for generating COGs, and user authentication (see [Figure 5](#)).

176 The front-end of the platform includes a landing page introducing users to the platform's features,
177 and a dataset page for searching and filtering the database through a list or world map. Users can
178 select a specific dataset to access the *details page*, which visualizes one orthophoto with correspond-
179 ing labels and their metadata. From here, users can download datasets without needing an account.
180 A second page visualizes large-scale satellite-based deadwood maps. Finally, a user-specific profile
181 page, which requires login, enables users to upload orthophotos and labels and manage their data.

182 Registered users can upload orthophotos, in the form of GeoTiffs, and labels to the system together
183 with a set of metadata data that includes the author names and acquisition date per orthophoto. Upon
184 successful submission to the system, additional metadata is generated, that is administrative level, file

185 size, file type. All metadata, along with vector labels, is stored in a cloud-hosted [Supabase](#) database,
186 which is accessible via Python and JavaScript client libraries. Data audit workflows require specific
187 user access levels, which are assigned to the deadtrees.earth core team. For user authentication, we
188 use Supabase Auth, which is based on JSON Web Tokens (JWTs). This ensures secure access while
189 integrating with Supabase's database features to implement Row Level Security (RLS), ensuring that
190 each user can only access data they are authorized to view.

191 To efficiently visualize a large collection of orthophotos with minimal resources, the platform
192 uses Cloud Optimized GeoTIFFs (COGs). COGs allow users to view and work with large orthopho-
193 tos quickly and efficiently, which is especially helpful when bandwidth or processing power is limited.
194 COGs are internally tiled and include overviews, making them accessible via HTTP range requests
195 without the need for server-side processing. This approach allows clients to fetch only the necessary
196 data, optimizing transfer and reducing server load. As a result, COGs significantly improve perfor-
197 mance compared to traditional Web Map Services (WMS) such as GeoServer or MapServer.

198 The resource-intensive generation of COGs is performed on a separate processing server. The
199 server periodically pulls user-uploaded GeoTIFF files from the storage server, performs the necessary
200 processing, and pushes the generated COGs back to the storage server (see [Figure 5](#)). A Python-based
201 REST API built with FastAPI manages processing tasks, user management, and resource allocation.
202 The front-end initiates tasks such as uploading, downloading, metadata generation, and processing
203 COGs through this REST API, which can also be used directly for programmatic data ingestion and
204 processing. The deadtrees.earth API also employs a queuing system to manage processes and prevent
205 downtime which ensures stability and scalability.

206 Finally, the platform's modular design allows for future integration of advanced workflows, such
207 as machine learning models for automated deadwood segmentation from drone imagery. By leverag-
208 ing powerful local processing servers, these workflows can be added seamlessly, making the platform
209 adaptable and flexible to meet evolving needs.

210 **2.4 Data Sources and Current State of the Database**

211 The primary sources for the orthophotos and labels are community contributions, *i.e.*, datasets that
212 individuals or institutions actively contributed. Given the large interest in monitoring tree mortality
213 dynamics worldwide, the deadtrees.earth database received tremendous support from a wide array of
214 individuals and institutions. So far, 87 institutions shared data across 67 countries.

215 **Crowd-Sourcing:** In addition to community contributions, the database integrates crowd-sourced
216 data, *i.e.*, datasets already freely available online. Indeed despite extensive community efforts to date,
217 significant portions of the Earth remain uncovered in our database. Therefore to maximize database
218 coverage, we integrate publicly available databases that adhere to appropriate licensing schemes.

219 While other initiatives, such as [GeoNadir](#), [OpenAerialMap](#), and [OpenDroneMap](#), also collect
220 drone orthophotos, only OpenAerialMap currently ensures that all contributions are licensed un-
221 der CC BY, making them suitable for use in projects like deadtrees.earth. As of June 2024, Ope-
222 nAerialMap hosts over 15,000 aerial orthophotos. We use this community-driven resource to expand
223 the deadtrees.earth database. However, most of the contributions to OpenAerialMap do not meet our
224 database criteria due to limitations in resolution, site relevance, quality, or acquisition timing. To be
225 able to extract usable images, we downloaded a summary of the metadata on 24th April 2024 through
226 their open API. Then we first filter the entries with where at least 30% is covered by forest accord-
227 ing to ESA Worldcover (Zanaga et al. 2022). To then remove orthophotos that lack the necessary
228 spatial resolution ([Figure 1](#)), we filtered images to include only resolutions better than 10 cm, yield-
229 ing 1102 samples. To only include orthophotos of forests within the growing season, we filtered the
230 months May to August for samples north of latitude 23.5°N, December to March for samples south of
231 latitude 23.5°S, and included all images for latitudes in between. Note that at a later stage we will dif-
232 ferentiate between wet and dry seasons for tropical region. Finally, we manually iterated through the
233 thumbnails or the original GeoTIFF of every orthophoto to visually check their quality. This resulted
234 in a final set of 448 (out of > 15,000 on OpenAerialMap) orthophotos with wide temporal (2007 to
235 2024) and geographic coverage (see [Figure 6](#)).

236 It is worth noting that the dataset extracted from OpenAerialMap has a bias towards forests near
237 human settlements, potentially over-representing ecosystems that might not be representative of the
238 region. For example, an orthophoto may contain 20 ha of a relevant forest, but another 100 ha of the
239 image contains a building site that the drone operator originally planned to capture. Nevertheless, this
240 crowd-sourced dataset provides valuable, high-resolution imagery of forests in ecosystems that would
241 otherwise not be part of our database. Additionally, this bias may provide an opportunity for studies
242 focusing on studying forest fragments and urban forests. As OpenAerialMap grows in the future, we
243 will continuously monitor their database for relevant submissions. Also, other relevant sources with a
244 CC-BY license will be integrated.

245 **Database Statistics:** We launch the seed database with 1,390 centimeter-scale orthophotos cover-

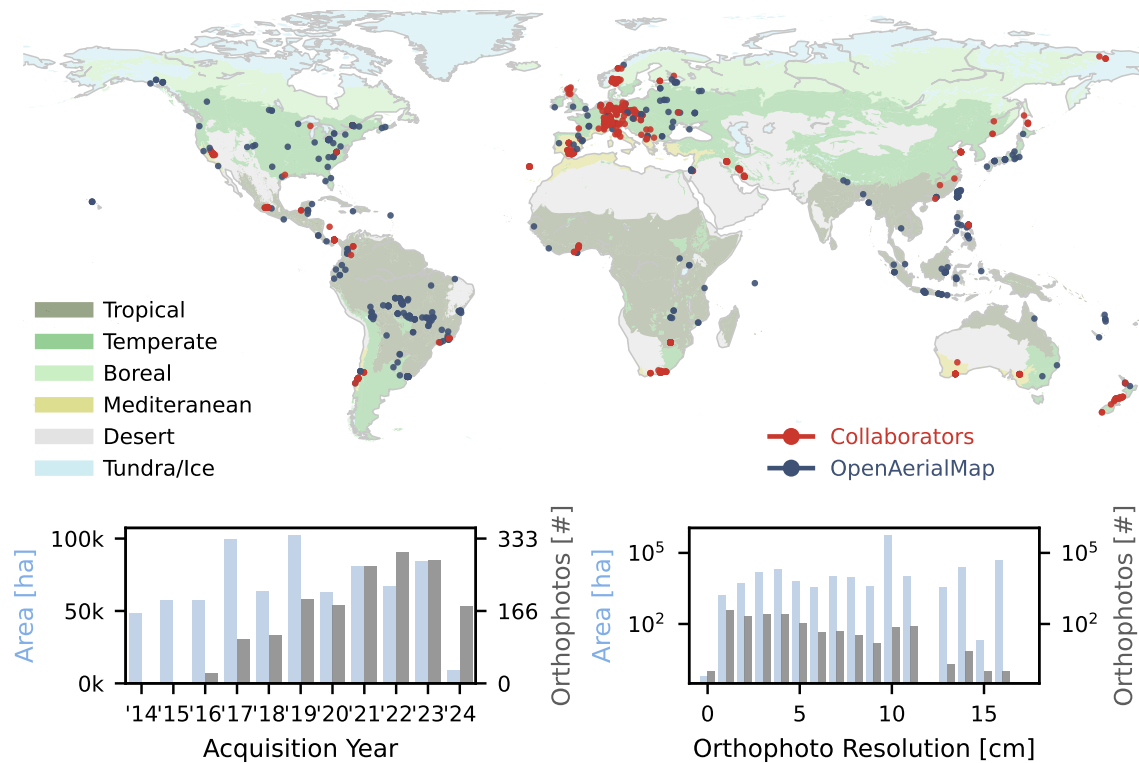


Figure 6: Initial statistics of the database upon launch depicting geographical, temporal, and resolution diversity. In the two bottom panels, drone orthophotos are accumulated by area (light blue) and count (dark gray). Different colors in the background depict different biomes (Olson et al. 2001).

246 ing 345,595 ha and spanning all continents (except Antarctica) through community contributions and
247 crowd-sourced data. By the time of submission (Oct. 2024), the database consists of 998 (71%) drone
248 orthophotos from community contributions and 392 (28%) crowd-sourced orthophotos extracted from
249 OpenAerialMap (Figure 6). The increasing ease of use of drones within the last decade is reflected
250 in the greater number of unique orthophotos in recent years. Additionally, the database includes 140
251 aerial images with resolutions less than 10 cm (Figure 6). Beyond local forest plots, we provide ac-
252 cess to aerial images with machine-learning generated tree mortality labels that were published on
253 our platform as the result of several studies (Cheng et al. 2024; Schwarz et al. 2024; Weinstein et al.
254 2024). These products cover the state of California (USA), Luxembourg, and 23 NEON sites in the
255 USA (not shown in Figure 6).

256 **Notable Collections:** Although a large part of the database consists of individual locations that
257 have been captured, it also features noteworthy collections that provide independent value, for exam-
258 ple through temporal coverage across multiple months or years. Notable collections include:

- 259 • **Barro Colorado Island (Panama)** 90 orthophotos capturing the same 50 ha plot across 6 years

260 (Vasquez et al. 2023).

261 • **Quebec (Canada)** Seven consecutive orthophotos of the same lake area from May to October
262 2021 (Cloutier et al. 2023, September).

263 • **Nationalpark Black Forest (Germany)** A 10-year timeseries covering the entire national park
264 (Christoph Dreiser).

265 • **Baden Wuerttemberg (Germany)** 135 unique plots (> 1 ha) in southwest Germany captured
266 in up to three different years, respectively ([ConFoBi](#)).

267 • **Andalucia (Spain)** 60 tree mortality sites (>15 ha) in otherwise protected national parks in
268 2023 (Clemens Mosig and Oscar Pérez-Priego).

269 • **Eastern Cape (South Africa)** 35 tree mortality sites captured between 2022 and 2024 provid-
270 ing unique data from Africa (Alastair Potts).

271 • **Zagros Forests (Iran)** 16 RGB Orthophotos captured in ca. 1 ha sample plots representing
272 *Quercus brantii* (oak) decline. Distributed over the large latitudinal gradient of semiarid Zagros
273 Forests in western Iran (Ghasemi et al. 2022, 2024a,b).

274 • **NIBIO UAV archive (Norway):** 50 UAV RGB orthophotos captured by NIBIO's Forest and
275 Forest Resource division between 2017 - 2022 using a variety of DJI drones. These data were
276 in collected primarily in south eastern Norway (Bhatnagar et al. 2022; Puliti et al. 2019, 2020).

277 The latter six collections have not been available to the public until now.

278 **Labels:** The database contains 54,320 *manually delineated* polygons delineating partial dieback,
279 individual trees or multiple dead tree crowns. In total, 493 orthophotos and 58,219 ha are fully la-
280 beled, of which 245 have quality 3/3, 231 have quality 2/3, and 5 orthophotos have quality 1/3 (see
281 [Subsection 2.2](#) for quality definition). These datasets will soon be available as machine learning ready
282 datasets (see Section [Section 3](#)) to support the community with training semantic or instance segmen-
283 tation models. At present, this unique data collection would result in more than 600.000 labeled
284 512x512 patches or 170.000 labeled 1024x1024 patches.

285 For this data collection we strictly adhere to the FAIR principle (Wilkinson et al. 2016). All data
286 is **F**indable, *i.e.*, has a unique identifier, is described with metadata, and thus searchable. Access is
287 provided through industry-standard and authentication-free HTTP requests on the website or pro-
288 grammatically (compare [Subsection 2.3](#)). We provide data **I**nteroperability by using GeoTIFF format

289 and standard datatypes for metadata (see [Figure 8](#)). Lastly, all data is **Reusable** as it is published under
290 a Creative Commons license.

291 In summary, through community efforts and crowd-sourcing of data, and to the best of our knowl-
292 edge, the [deadtrees.earth](#) database curates an unprecedented amount of super-resolution optical im-
293 agery and corresponding labels. With the increasing recognition of this database and the general
294 growing willingness for open data in science and the public, we expect this database to continue
295 expanding rapidly.

296 **3 Outlook and Perspective**

297 **3.1 Database Expansion Through Community Contribution**

298 Excess tree mortality is a global phenomenon whose underlying complexity can only be effectively
299 assessed through community effort (The International Tree Mortality Network et al. 2024). The
300 [deadtrees.earth](#) platform initiates with a collection of centimeter-scale forest orthophotos that is al-
301 ready orders of magnitude larger in spatial coverage and diversity than in any mortality-related study
302 used. However, this collection is biased towards the Global North, and regions in Asia and Africa are
303 particularly underrepresented (see [Figure 6](#)). As we aim to grow into a representative collection of
304 tree mortality in the World's forest ecosystems, we require a more diverse collection of orthophotos.
305 We therefore encourage everyone in every community to take the opportunity to participate in this
306 global initiative.

307 In the primary use case, a contributor submits an orthophoto covering any forest with a resolution
308 better than 10 cm. Optionally, delineated standing deadwood can be submitted as shapefiles or sim-
309 ilar formats. Beyond that, we also welcome lower-resolution aerial images with already delineated
310 standing deadwood. These delineations can be manually obtained or also the product of automated
311 segmentation, and need to be declared as such, *e.g.*, the results of Cheng et al. 2024 are available in
312 the database. The orthophotos do not necessarily need to contain large or any fractions of standing
313 deadwood, as the machine learning models have to be trained on alive and dead trees. Since anyone
314 can submit data to the database, a database manager manually reviews the supplied metadata and the
315 geolocation of the orthophoto and, if available, grades the quality of the submitted label set. This
316 ensures that the database continues to grow without barriers while maintaining the highest possible
317 quality.

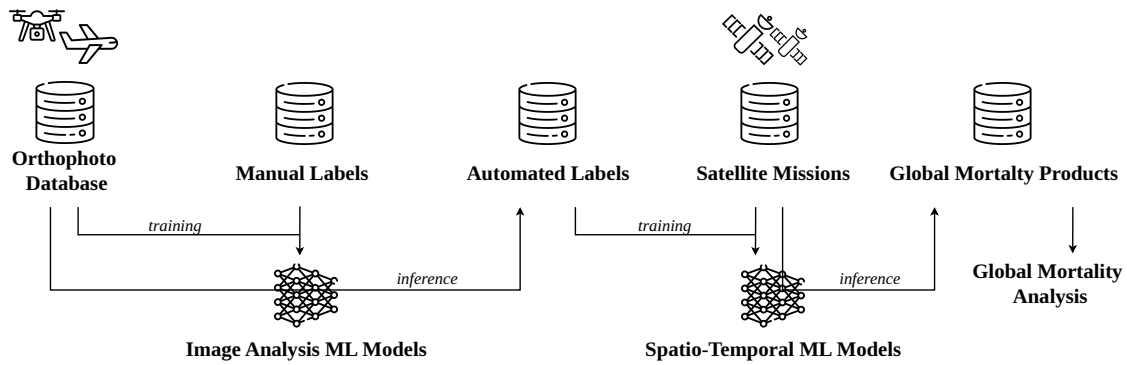


Figure 7: Generalized workflow to derive a global tree mortality product through the deadtrees.earth database.

318 Newly submitted orthophotos of local tree mortality events bolster the global and temporal repre-
319 sentativeness of the database. This is critical for training models that aim for a global transferability
320 (Kattenborn et al. 2022; Meyer and Pebesma 2022), be it computer vision models that segment dead
321 trees in drone data or satellite-based models. Hence, an individual submission of a user’s local forest
322 can be an important missing puzzle piece in creating a representative training dataset. Subsequently,
323 machine-learning models will improve in the user’s local region, providing a strong incentive to con-
324 tribute their data as they indirectly benefit.

325 3.2 Towards Tree Mortality Models and Products from Local to Global Scale

326 Delineated standing deadwood identified from large amounts of centimeter-scale orthophotos is a
327 powerful data source for creating high-precision training data. Deadtrees.earth provides a unique
328 dataset that will enable the machine-learning community to create models and maps that are transfer-
329 able at a global scale and robust across the diversity of forest ecosystems (Figure 7).

330 Given the rich database presented here, users can train various types of **computer vision models**
331 **for identifying standing deadwood in drone orthoimagery**, *e.g.*, in the form of semantic segmen-
332 tation (polygons of dead crowns, twigs or branches), object detection (bounding boxes of individ-
333 ual trees), or instance segmentation (precise crowns of individual trees). With such models, one can
334 perform inference on all orthophotos in the database to automatically reveal the local distributions
335 of standing deadwood. This is particularly relevant for orthophotos that do not have labels from a
336 human interpreter. Machine-learning-based predictions may even be advantageous over labels from
337 human interpreters as they might be more standardized and objective (in contrast to manually delin-
338 eated polygons from different human interpreters). This automated mapping of standing deadwood

339 is also meant to be one of the core incentives for users interacting with the deadtrees.earth. Thus,
340 deadtrees.earth will provide a hub for making machine-learning-based technology developed by the
341 community accessible for non-experts (*e.g.*, practitioners, citizens, Non-government organizations)
342 or people with limited resources.

343 The local patterns of standing deadwood derived from orthophotos can be used as a reference
344 for **large-scale machine-learning-based mapping using satellite data** from Sentinel, Landsat, or
345 future satellite missions. While Landsat and Sentinel data are much coarser in resolution than drone
346 data, approximately 10 m to 30 m, respectively, they have the advantage of having global coverage
347 and being multi-spectral data. The temporal continuity of Sentinel or Landsat data supports the cre-
348 ation of accurate global products, as machine-learning models can harness the temporal and spectral
349 patterns. For example, in optical satellite imagery, standing deadwood may look visually similar to a
350 grayish forest floor or rocks ([Figure 1](#)). However, in a time series of multiple years, a dead tree can be
351 differentiated from a forest floor or rocks based on its spectral history (Schiefer et al. 2023). This way,
352 deadtrees.earth will provide satellite-based models and predictions at a global scale in the future.

353 To stimulate the development of machine-learning models for analyzing drone and satellite data,
354 deadtrees.earth will provide ML-ready datasets, *e.g.*, integrated into the [torchgeo](#) library (Stewart et
355 al. 2022). This will enable the community to develop and benchmark different methods effectively.
356 Incentives for this might be further propelled by related coding competitions. Moreover, the machine-
357 learning-ready datasets will enable the development of workflows that are directly compatible with
358 the deadtrees.earth ecosystem, so that models and workflows developed in the community can be
359 directly integrated as an application.

360 With the launch of [deadtrees.earth](#) we aim to attract a variety of communities to this multi-
361 faceted platform. Through simple, interactive visualizations of orthophotos together with labels and
362 satellite-derived products on the website, we truly enable anyone to explore our and others' tree
363 mortality-related products. Viewing centimeter-scale imagery and satellite products side-by-side will
364 enable benchmarks, validation, and finally an understanding of large-scale patterns of forest mortal-
365 ity. In a citizen science approach, non-specialists can also contribute data without prior knowledge
366 of machine-learning methods used for further processing by us and the broad scientific community.
367 In the future, we aim to further increase participation on [deadtrees.earth](#) by enabling users to delin-
368 eate standing deadwood manually, correct AI segmentation outputs, and flag faulty predictions in the
369 satellite data.

370 **3.3 Applications of Global Tree Mortality Products**

371 Global, high-quality tree mortality products can be used with environmental layers to attribute mor-
372 tality dynamics to respective drivers and understand the variation in tree mortality dynamics. The
373 variety of global tree mortality products that can be derived from the database will be a key compo-
374 nent in enabling researchers to answer pressing questions: *Why are trees dying in the first place and*
375 *how do the drivers (co)vary across tree species, ecosystems, or biomes? Why do some areas experi-*
376 *ence excess tree mortality while similar areas experience greening? Is tree mortality dependent upon*
377 *the species or diversity of neighboring trees? What is the anthropogenic contribution to excess tree*
378 *mortality? How long does standing deadwood remain in different ecosystems and does this relate to*
379 *large-scale carbon balances? Where can tree mortality be attributed to global warming and climate*
380 *extremes? Do the latter factors facilitate (invasive) pests and pathogens?* Given high product quality
381 and increasing global coverage, we hope to support research on tree mortality from a local to a global
382 scale and across biomes.

383 For example, one can combine standing deadwood maps with large-scale biomass maps (San-
384 toro et al. 2020; Shendryk 2022) to facilitate our understanding of carbon fluxes. Given the tem-
385 poral dynamics of standing deadwood, we can compare results to the outputs of vegetation models
386 (*e.g.*, (Köhler and Huth 1998)). Thereby, using remote sensing derived products to evaluate and also
387 fine-tune or initialize parameterizations of vegetation models. Beyond Now- and Hindcasting, Fore-
388 casting of tree mortality should be possible if the community finds effective environmental predictors
389 such that tree mortality dynamics for the subsequent year can be modeled.

390 Beyond tree mortality applications, we envision the orthophoto database to be used in a variety
391 of other use cases. Since in general, this is a centimeter-scale orthophoto database of forests, one can
392 also attempt to detect tree species, analyze tree line patterns, derive tree/non-tree products, pioneer
393 studies on tree health, tree phenology, or attempt to track forest cover dynamics. Broadly speaking the
394 general workflow (see [Figure 7](#)) of upscaling to global products can also be attempted for the same
395 use cases. Especially suited may be forest cover products, tree species distribution maps, or revealing
396 tree loss by forest management or windthrows.

397 **4 Conclusions**

398 The deadtrees.earth database is a centimeter-scale orthophoto collection with standing deadwood de-
399 lineations. Already, it comprises 1,390 centimeter-scale orthophotos with more than 55,000 deadwood
400 labels from the last decade distributed across the entire globe. The dataset has unprecedented cover-
401 age, and through machine learning methods and global remote sensing satellite missions, the scientific
402 community can leverage this dataset to create models and global datasets, unlocking the potential to
403 effectively track tree mortality dynamics. Ultimately, these data in concert with environmental layers
404 will enable the scientific community to answer pressing questions on tree mortality. To reach this goal,
405 the platform www.deadtrees.earth encompasses an interactive online system that aims to exploit aerial
406 and satellite imagery for uncovering spatial and temporal patterns of tree mortality at a global scale.
407 The web platform supports and encourages uploading and downloading user-generated orthophotos
408 optionally together with labeled standing deadwood. The vision of this platform is an improved un-
409 derstanding of tree mortality patterns and processes from local to global scales. And this vision can
410 only be accomplished through the collective effort of citizens and researchers. The dynamic nature of
411 this database is meant to continuously increase our capacity to detect and understand tree mortality
412 patterns. We hope that through the services of deadtrees.earth, we can attract ample data input from
413 geographic regions that are currently still underrepresented (*e.g.*, the global south). Finally, with this
414 initiative, we support the paradigm shift in data-sharing practices in the scientific community.

415 **Acknowledgements**

416 The study has been funded by the German Aerospace Centre (DLR) on behalf of the Federal Min-
417 istry for Economic Affairs and Climate Action (BMWK) under the projects *UAVforSAT* (project no.
418 50EE1909A) and *ML4Earth* (FKZ 50EE2201B). Further funding was received from the German
419 Research Foundation (DFG) under the project *BigPlantSens* (project no. 444524904) and PANOPS
420 (project no. 504978936). Further funding was received from the Ministry of Food, Rural Areas and
421 Consumer Protection under the project PRIMA (project no. 52-8670.00). Some of the icons were
422 provided by Flaticon. JF acknowledges funding by the German Research Foundation (DFG Project
423 ConFobi, GRK 2123). CM, MDM, and JU acknowledge the financial support by the Federal Min-
424 istry of Education and Research of Germany and by Sächsische Staatsministerium für Wissenschaft,

425 Kultur und Tourismus in the programme Center of Excellence for AI-research, Center for Scalable
 426 Data Analytics and Artificial Intelligence Dresden/Leipzig, project identification number: ScaDS.AI.
 427 CM and MDM thank the European Space Agency for funding the “DeepFeatures” project via the
 428 AI4SCIENCE activity. SH and YC are funded by Villum Fonden (DRYTIP project, grant agree-
 429 ment no. 37465) and the University of Copenhagen (PerformLCA project, UCPH Strategic plan
 430 2023 Data+ Pool). We acknowledge the Black Forest National Park Administration as on of the data
 431 providers. The research of KCC was carried out at Oak Ridge National Laboratory, which is man-
 432 aged by the University of Tennessee-Battelle, LLC, under contract DE-AC05-00OR22725 with the
 433 U.S. Department of Energy. This study was supported by the International Tree Mortality Network
 434 (<https://tree-mortality.net/>).

435 Supplementary Material

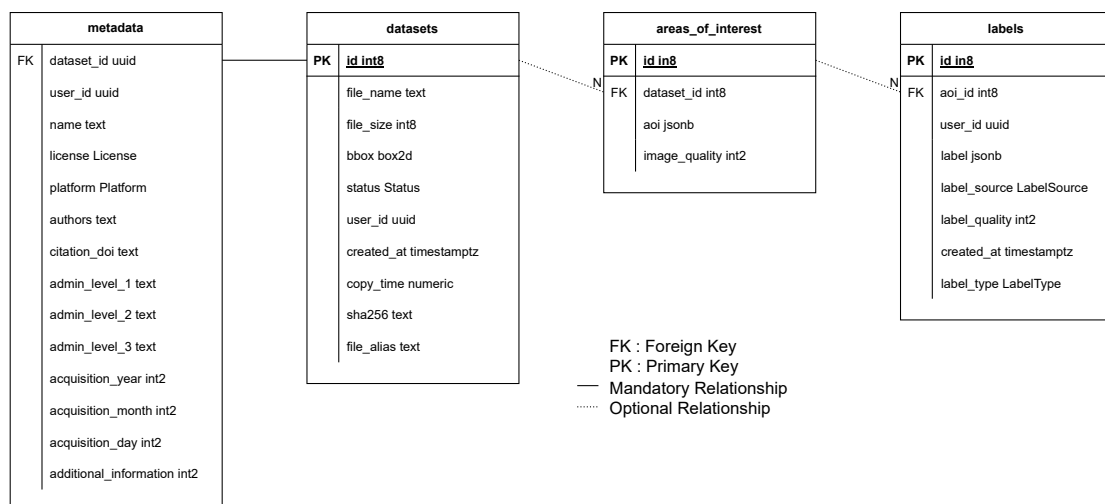


Figure 8: Full relational diagram of the deadtrees.earth database.

436 Conflicts of Interest Statement

437 All authors declare that they have no conflicts of interest.

438 **Author contributions**

439 Conceptualization: C. Mosig, T. Kattenborn, and J. Vajna-Jehle. Writing - original draft: C. Mosig
440 and T. Kattenborn. Writing - review & editing: C. Mosig, Y. Cheng, J. Vajna-Jehle, S. Junntila, T. Kat-
441 tenborn, H. Hartmann, S. Horion, M. D. Mahecha, D. Montero, M. B. Schwenke. Analysis and Visu-
442 alization: C. Mosig, T. Kattenborn, and J. Vajna-Jehle. Platform development (front-end, back-end):
443 J. Vajna-Jehle, M. Mälicke, C. Mosig. All others contributed data, revised the manuscript, and gave
444 approval for publication.

445 **References**

- 446 Allen, C. D., Breshears, D. D., & McDowell, N. G. (2015). On underestimation of global vulnerability
447 to tree mortality and forest die-off from hotter drought in the anthropocene. *Ecosphere*, 6(8),
448 1–55.
- 449 Allen, C. D., Macalady, A. K., Chenchouni, H., Bachelet, D., McDowell, N., Vennetier, M., Kitzberger,
450 T., Rigling, A., Breshears, D. D., Hogg, E. T., et al. (2010). A global overview of drought and
451 heat-induced tree mortality reveals emerging climate change risks for forests. *Forest ecology
452 and management*, 259(4), 660–684.
- 453 Anderegg, W. R., Kane, J. M., & Anderegg, L. D. (2013). Consequences of widespread tree mortality
454 triggered by drought and temperature stress. *Nature climate change*, 3(1), 30–36.
- 455 Bastos, A., Sippel, S., Frank, D., Mahecha, M. D., Zaehle, S., Zscheischler, J., & Reichstein, M.
456 (2023). A joint framework for studying compound ecoclimatic events. *Nature Reviews Earth
457 & Environment*, 4(5), 333–350.
- 458 Bauman, D., Fortunel, C., Delhay, G., Malhi, Y., Cernusak, L. A., Bentley, L. P., Rifai, S. W.,
459 Aguirre-Gutiérrez, J., Menor, I. O., Phillips, O. L., et al. (2022). Tropical tree mortality has
460 increased with rising atmospheric water stress. *Nature*, 608(7923), 528–533.
- 461 Bhatnagar, S., Puliti, S., Talbot, B., Heppelmann, J. B., Breidenbach, J., & Astrup, R. (2022). Map-
462 ping wheel-ruts from timber harvesting operations using deep learning techniques in drone
463 imagery. *Forestry*, 95(5), 698–710.

- 464 Cheng, Y., Oehmcke, S., Brandt, M., Rosenthal, L., Das, A., Vrieling, A., Saatchi, S., Wagner, F.,
465 Mugabowindekwe, M., Verbruggen, W., et al. (2024). Scattered tree death contributes to sub-
466 stantial forest loss in california. *Nature communications*, *15*(1), 641.
- 467 Cloutier, M., Germain, M., & Laliberté, E. (2023, September). *Quebec trees dataset*. Zenodo. <https://doi.org/10.5281/zenodo.8148479>
468
- 469 Coleman, T. W., Graves, A. D., Heath, Z., Flowers, R. W., Hanavan, R. P., Cluck, D. R., & Ryerson,
470 D. (2018). Accuracy of aerial detection surveys for mapping insect and disease disturbances
471 in the united states. *Forest ecology and management*, *430*, 321–336.
- 472 Dandois, J. P., Olano, M., & Ellis, E. C. (2015). Optimal altitude, overlap, and weather conditions for
473 computer vision uav estimates of forest structure. *Remote sensing*, *7*(10), 13895–13920.
- 474 Espírito-Santo, F. D., Gloor, M., Keller, M., Malhi, Y., Saatchi, S., Nelson, B., Junior, R. C. O.,
475 Pereira, C., Lloyd, J., Frohking, S., et al. (2014). Size and frequency of natural forest distur-
476 bances and the amazon forest carbon balance. *Nature communications*, *5*(1), 1–6.
- 477 Fettig, C., Mortenson, L., Bulaon, B., & Foulk, P. (2019). Tree mortality following drought in the
478 central and southern sierra nevada, california, us for. *ecol. manage.* *432*, 164–178.
- 479 Frey, J., Kovach, K., Stemmler, S., & Koch, B. (2018). Uav photogrammetry of forests as a vulner-
480 able process. a sensitivity analysis for a structure from motion rgb-image pipeline. *Remote*
481 *Sensing*, *10*(6), 912.
- 482 Garrity, S. R., Allen, C. D., Brumby, S. P., Gangodagamage, C., McDowell, N. G., & Cai, D. M.
483 (2013). Quantifying tree mortality in a mixed species woodland using multitemporal high
484 spatial resolution satellite imagery. *Remote Sensing of Environment*, *129*, 54–65.
- 485 Ghasemi, M., Latifi, H., & Pourhashemi, M. (2022). A novel method for detecting and delineating
486 coppice trees in uav images to monitor tree decline. *Remote Sensing*, *14*(23), 5910.
- 487 Ghasemi, M., Latifi, H., & Pourhashemi, M. (2024a). Integrating uav and freely available space-borne
488 data to describe tree decline across semi-arid mountainous forests. *Environmental Modeling*
489 *& Assessment*, *29*(3), 549–568.
- 490 Ghasemi, M., Latifi, H., Shafeian, E., Naghavi, H., & Pourhashemi, M. (2024b). A novel linear spec-
491 tral unmixing-based method for tree decline monitoring by fusing uav-rgb and optical space-
492 borne data. *International Journal of Remote Sensing*, *45*(4), 1079–1109.
- 493 Gora, E. M., & Esquivel-Muelbert, A. (2021). Implications of size-dependent tree mortality for trop-
494 ical forest carbon dynamics. *Nature Plants*, *7*(4), 384–391.

- 495 Hammond, W. M., Williams, A. P., Abatzoglou, J. T., Adams, H. D., Klein, T., López, R., Sáenz-
496 Romero, C., Hartmann, H., Breshears, D. D., & Allen, C. D. (2022). Global field observations
497 of tree die-off reveal hotter-drought fingerprint for earth's forests. *Nature Communications*,
498 *13*(1), 1761.
- 499 Hansen, M. C., Potapov, P. V., Moore, R., Hancher, M., Turubanova, S. A., Tyukavina, A., Thau,
500 D., Stehman, S. V., Goetz, S. J., Loveland, T. R., Kommareddy, A., Egorov, A., Chini, L.,
501 Justice, C. O., & Townshend, J. R. G. (2013). High-resolution global maps of 21st-century
502 forest cover change. *Science*, *342*(6160), 850–853. <https://doi.org/10.1126/science.1244693>
- 503 Hartmann, H., Bastos, A., Das, A. J., Esquivel-Muelbert, A., Hammond, W. M., Martínez-Vilalta, J.,
504 McDowell, N. G., Powers, J. S., Pugh, T. A., Ruthrof, K. X., et al. (2022). Climate change
505 risks to global forest health: Emergence of unexpected events of elevated tree mortality world-
506 wide. *Annual Review of Plant Biology*, *73*, 673–702.
- 507 Hill, A. P., Nolan, C. J., Hemes, K. S., Cambron, T. W., & Field, C. B. (2023). Low-elevation conifers
508 in california's sierra nevada are out of equilibrium with climate. *PNAS nexus*, *2*(2), pgad004.
- 509 Hülsmann, L., Bugmann, H., & Brang, P. (2017). How to predict tree death from inventory data—lessons
510 from a systematic assessment of european tree mortality models. *Canadian Journal of Forest*
511 *Research*, *47*(7), 890–900.
- 512 Johnson, P., Ricker, B., & Harrison, S. (2017). Volunteered drone imagery: Challenges and constraints
513 to the development of an open shared image repository.
- 514 Junttila, S., Blomqvist, M., Laukkanen, V., Heinaro, E., Polvivaara, A., O'Sullivan, H., Yrttimaa,
515 T., Vastaranta, M., & Peltola, H. (2024). Significant increase in forest canopy mortality in
516 boreal forests in southeast finland. *Forest Ecology and Management*, *565*, 122020. <https://doi.org/https://doi.org/10.1016/j.foreco.2024.122020>
- 517
- 518 Kattenborn, T., Schiefer, F., Frey, J., Feilhauer, H., Mahecha, M. D., & Dormann, C. F. (2022). Spa-
519 tially autocorrelated training and validation samples inflate performance assessment of con-
520 volutional neural networks. *ISPRS Open Journal of Photogrammetry and Remote Sensing*, *5*,
521 100018.
- 522 Köhler, P., & Huth, A. (1998). The effects of tree species grouping in tropical rainforest modelling:
523 Simulations with the individual-based model formind. *Ecological Modelling*, *109*(3), 301–
524 321.

- 525 Lange, M., Preidl, S., Reichmuth, A., Heurich, M., & Doktor, D. (2024). A continuous tree species-
526 specific reflectance anomaly index reveals declining forest condition between 2016 and 2022
527 in Germany. *Remote Sensing of Environment*, 312, 114323.
- 528 Mahecha, M. D., Bastos, A., Bohn, F., Eisenhauer, N., Feilhauer, H., Hickler, T., Kalesse-Los, H.,
529 Migliavacca, M., Otto, F. E. L., Peng, J., et al. (2024). Biodiversity and climate extremes:
530 Known interactions and research gaps. *Earth's Future*, 12(6), e2023EF003963.
- 531 McRoberts, R. E., Tomppo, E. O., & Næsset, E. (2010). Advances and emerging issues in national
532 forest inventories. *Scandinavian Journal of Forest Research*, 25(4), 368–381.
- 533 Meyer, H., & Pebesma, E. (2022). Machine learning-based global maps of ecological variables and
534 the challenge of assessing them. *Nature Communications*, 13(1), 2208.
- 535 Moghaddas, J., Roller, G., Long, J., Saah, D., Moritz, M., Star, D., Schmidt, D., Buchholz, T., Freed,
536 T., Alvey, E., et al. (2018). Fuel treatment for forest resilience and climate mitigation: A crit-
537 ical review for coniferous forests of california. *California Natural Resources Agency. Publi-*
538 *cation number: CCCA4-CNRA-2018-017.*
- 539 Olson, D. M., Dinerstein, E., Wikramanayake, E. D., Burgess, N. D., Powell, G. V. N., Underwood,
540 E. C., D'amico, J. A., Itoua, I., Strand, H. E., Morrison, J. C., Loucks, C. J., Allnutt, T. F.,
541 Ricketts, T. H., Kura, Y., Lamoreux, J. F., Wettengel, W. W., Hedao, P., & Kassem, K. R.
542 (2001). Terrestrial Ecoregions of the World: A New Map of Life on Earth: A new global map
543 of terrestrial ecoregions provides an innovative tool for conserving biodiversity. *BioScience*,
544 51(11), 933–938. [https://doi.org/10.1641/0006-3568\(2001\)051\[0933:TEOTWA\]2.0.CO;2](https://doi.org/10.1641/0006-3568(2001)051[0933:TEOTWA]2.0.CO;2)
- 545 Pan, Y., Birdsey, R. A., Fang, J., Houghton, R., Kauppi, P. E., Kurz, W. A., Phillips, O. L., Shvidenko,
546 A., Lewis, S. L., Canadell, J. G., et al. (2011). A large and persistent carbon sink in the world's
547 forests. *Science*, 333(6045), 988–993.
- 548 Puletti, N., Canullo, R., Mattioli, W., Gawryś, R., Corona, P., & Czerepko, J. (2019). A dataset of
549 forest volume deadwood estimates for europe. *Annals of Forest Science*, 76, 1–8.
- 550 Puliti, S., Breidenbach, J., & Astrup, R. (2020). Estimation of forest growing stock volume with uav
551 laser scanning data: Can it be done without field data? *Remote Sensing*, 12(8), 1245.
- 552 Puliti, S., Solberg, S., & Granhus, A. (2019). Use of uav photogrammetric data for estimation of
553 biophysical properties in forest stands under regeneration. *Remote Sensing*, 11(3), 233.

- 554 Rossi, C., & Wiesmann, S. (2024). Flying high for conservation: Opportunities and challenges of op-
555 erating drones within the oldest national park in the alps. *Ecological Solutions and Evidence*,
556 5(2), e12354.
- 557 Santoro, M., Cartus, O., Carvalhais, N., Rozendaal, D., Avitabile, V., Araza, A., De Bruin, S., Herold,
558 M., Quegan, S., Rodríguez Veiga, P., et al. (2020). The global forest above-ground biomass
559 pool for 2010 estimated from high-resolution satellite observations. *Earth System Science*
560 *Data Discussions*, 2020, 1–38.
- 561 Scheffer, M., Carpenter, S., Foley, J. A., Folke, C., & Walker, B. (2001). Catastrophic shifts in ecosys-
562 tems. *Nature*, 413(6856), 591–596.
- 563 Schiefer, F., Schmidlein, S., Frick, A., Frey, J., Klinke, R., Zielewska-Büttner, K., Junttila, S., Uhl,
564 A., & Kattenborn, T. (2023). Uav-based reference data for the prediction of fractional cover
565 of standing deadwood from sentinel time series. *ISPRS Open Journal of Photogrammetry*
566 *and Remote Sensing*, 8, 100034.
- 567 Schiefer, F., Schmidlein, S., Hartmann, H. H., Schnabel, F., & Kattenborn, T. (2024). Large-scale
568 remote sensing reveals that tree mortality in germany appears to be greater than previously
569 expected. *Under Review*.
- 570 Schwarz, S., Werner, C., Fassnacht, F. E., & Ruehr, N. K. (2024). Forest canopy mortality during
571 the 2018-2020 summer drought years in central europe: The application of a deep learning
572 approach on aerial images across luxembourg. *Forestry: An International Journal of Forest*
573 *Research*, 97(3), 376–387.
- 574 Senf, C., Buras, A., Zang, C. S., Rammig, A., & Seidl, R. (2020). Excess forest mortality is consis-
575 tently linked to drought across europe. *Nature communications*, 11(1), 6200.
- 576 Senf, C., Pflugmacher, D., Zhiqiang, Y., Sebald, J., Knorn, J., Neumann, M., Hostert, P., & Seidl,
577 R. (2018). Canopy mortality has doubled in europe’s temperate forests over the last three
578 decades. *Nature Communications*, 9(1), 4978.
- 579 Senf, C., & Seidl, R. (2021). Mapping the forest disturbance regimes of europe. *Nature Sustainability*,
580 4(1), 63–70.
- 581 Shendryk, Y. (2022). Fusing gedi with earth observation data for large area aboveground biomass
582 mapping. *International Journal of Applied Earth Observation and Geoinformation*, 115,
583 103108.

- 584 Stephens, S. L., Bernal, A. A., Collins, B. M., Finney, M. A., Lautenberger, C., & Saah, D. (2022).
585 Mass fire behavior created by extensive tree mortality and high tree density not predicted by
586 operational fire behavior models in the southern sierra nevada. *Forest Ecology and Manage-*
587 *ment*, 518, 120258.
- 588 Stephens, S. L., Collins, B. M., Fettig, C. J., Finney, M. A., Hoffman, C. M., Knapp, E. E., North,
589 M. P., Safford, H., & Wayman, R. B. (2018). Drought, tree mortality, and wildfire in forests
590 adapted to frequent fire. *BioScience*, 68(2), 77–88.
- 591 Stephenson, N. L., Das, A. J., Ampersee, N. J., Bulaon, B. M., & Yee, J. L. (2019). Which trees die
592 during drought? the key role of insect host-tree selection. *Journal of Ecology*, 107(5), 2383–
593 2401.
- 594 Stewart, A. J., Robinson, C., Corley, I. A., Ortiz, A., Ferres, J. M. L., & Banerjee, A. (2022). Torch-
595 geo: Deep learning with geospatial data. *Proceedings of the 30th international conference on*
596 *advances in geographic information systems*, 1–12.
- 597 Tang, L., & Shao, G. (2015). Drone remote sensing for forestry research and practices. *Journal of*
598 *forestry research*, 26, 791–797.
- 599 The International Tree Mortality Network, Senf, C., Esquivel-Muelbert, A., Pugh, T. A. M., An-
600 deregg, W. R. L., Anderson-Teixeira, K. J., Arellano, G., Beloiu Schwenke, M., Bentz, B. J.,
601 Boehmer, H. J., Bond-Lamberty, B., Bordin, K., Boson De Castro-Faria, A., Brearley, F. Q.,
602 Bussotti, F., Cailleret, M., Camarero, J. J., Chirici, G., Costa, F. R., . . . Zuleta, D. (2024).
603 Towards a global understanding of tree mortality. *Under Review*.
- 604 Thonfeld, F., Gessner, U., Holzwarth, S., Kriese, J., da Ponte, E., Huth, J., & Kuenzer, C. (2022). A
605 first assessment of canopy cover loss in germany’s forests after the 2018–2020 drought years.
606 *Remote Sensing*, 14(3). <https://doi.org/10.3390/rs14030562>
- 607 Trugman, A. T., Anderegg, L. D., Anderegg, W. R., Das, A. J., & Stephenson, N. L. (2021). Why is
608 tree drought mortality so hard to predict? *Trends in Ecology & Evolution*, 36(6), 520–532.
- 609 Trumbore, S., Brando, P., & Hartmann, H. (2015). Forest health and global change. *Science*, 349(6250),
610 814–818.
- 611 Vasquez, V., Garcia, M., Hernandez, M., & Muller-Landau, H. C. (2023). Barro Colorado Island 50-
612 ha plot aerial photogrammetry orthomosaics and digital surface models for 2018-2023: Glob-
613 ally and locally aligned time series. [https://smithsonian.figshare.com/articles/dataset/Barro-](https://smithsonian.figshare.com/articles/dataset/Barro_Colorado_Island_50-ha_plot_aerial_photogrammetry_orthomosaics_and_digital_surface_models_)
614 [Colorado_Island_50-ha_plot_aerial_photogrammetry_orthomosaics_and_digital_surface_models_](https://smithsonian.figshare.com/articles/dataset/Barro_Colorado_Island_50-ha_plot_aerial_photogrammetry_orthomosaics_and_digital_surface_models_)

- 615 [for_2018 - 2023_Globally_and_locally_aligned_time_series_/24782016%20%22,%20doi%20=](#)
616 [%20%2210.25573/data.24782016.v1](#)
- 617 Vilanova, E., Mortenson, L. A., Cox, L. E., Bulaon, B. M., Lydersen, J. M., Fettig, C. J., Battles, J. J.,
618 & Axelson, J. N. (2023). Characterizing ground and surface fuels across sierra nevada forests
619 shortly after the 2012–2016 drought. *Forest Ecology and Management*, 537, 120945.
- 620 Watt, M. S., Holdaway, A., Watt, P., Pearse, G. D., Palmer, M. E., Steer, B. S. C., Camarretta, N.,
621 McLay, E., & Fraser, S. (2024). Early prediction of regional red needle cast outbreaks using
622 climatic data trends and satellite-derived observations. *Remote Sensing*, 16(8). [https://doi.](https://doi.org/10.3390/rs16081401)
623 [org/10.3390/rs16081401](https://doi.org/10.3390/rs16081401)
- 624 Weinstein, B. G., Marconi, S., Zare, A., Bohlman, S. A., Singh, A., Graves, S. J., Magee, L., Johnson,
625 D. J., Record, S., Rubio, V. E., et al. (2024). Individual canopy tree species maps for the
626 national ecological observatory network. *Plos Biology*, 22(7), e3002700.
- 627 Wilkinson, M. D., Dumontier, M., Aalbersberg, I. J., Appleton, G., Axton, M., Baak, A., Blomberg,
628 N., Boiten, J.-W., da Silva Santos, L. B., Bourne, P. E., et al. (2016). The fair guiding princi-
629 ples for scientific data management and stewardship. *Scientific data*, 3(1), 1–9.
- 630 Winter, C., Mueller, S., Kattenborn, T., Stahl, K., Szillat, K., Weiler, M., & Schnabel, F. (2024).
631 Forest dieback in drinking water protection areas—a hidden threat to water quality. *bioRxiv*,
632 2024–08.
- 633 Woodall, C., Grambsch, P., & Thomas, W. (2005). Applying survival analysis to a large-scale for-
634 est inventory for assessment of tree mortality in minnesota. *Ecological Modelling*, 189(1-2),
635 199–208.
- 636 Yan, Y., Piao, S., Hammond, W. M., Chen, A., Hong, S., Xu, H., Munson, S. M., Myneni, R. B., &
637 Allen, C. D. (2024). Climate-induced tree-mortality pulses are obscured by broad-scale and
638 long-term greening. *Nature Ecology & Evolution*, 8(5), 912–923.
- 639 Zanaga, D., Van De Kerchove, R., Daems, D., De Keersmaecker, W., Brockmann, C., Kirches, G.,
640 Wevers, J., Cartus, O., Santoro, M., Fritz, S., et al. (2022). Esa worldcover 10 m 2021 v200.